ISSN 0027-1314, Moscow University Chemistry Bulletin, 2007, Vol. 62, No. 3, pp. 132–135. © Allerton Press, Inc., 2007.
Original Russian Text © A.V. Mugtasimov, P.A. Chernavskii, 2007, published in Vestnik Moskovskogo Universiteta. Khimiya, 2007, No. 3, pp. 162–166.

Influence of Oxidation–Reduction Treatment on the Formation of Cobalt Nanoparticles in the Zr–Co–H System

A. V. Mugtasimov and P. A. Chernavskii

Physical Chemistry Department
e-mail: chern@kge.msu.ru

Received February 16, 2006

Abstract—Continuous in situ magnetization measurements are used to study the dynamics of processes in the Zr–Co–H system during oxidation–reduction treatment (ORT). The oxidation of a $ZrCoH_x$ sample after removal of hydrogen results in a significant rise in magnetization. $ZrCoH_x$ oxidation in air leads to higher magnetizations compared to oxidation in a 5% O_2 + Ar mixture.

DOI: 10.3103/S0027131407030042

Intermetallic hydrides (IMHs) are of interest for use as the base of hydrogenation catalytic systems, in particular, for Fischer–Tropsch synthesis. Intermetallic hydrides per se are not catalytically active. They acquire such activity when subjected to oxidation–reduction treatment (ORT) as a result of the segregation of one of their metals during ORT. The resulting metal nanoparticles are the catalytically active component [1].

Hydrides $ZrCoH_x$ deserve special consideration. First, cobalt-base Fischer–Tropsch catalysts are most selective to C_5 and higher liquid hydrocarbons. Second, nonstoichoimetric ZrO_2 is the promoter for some cobalt-base catalytic systems supported on Al_2O_3, SiO_2, or TiO_2. Third, the hydride system is conserved under sufficiently mild ORT parameters; for this reason, IMH-base catalysts have unique properties, such as the nonexistence of surface carbonization and the high concentrations of active surface hydrogen.

In order to prepare Fischer–Tropsch catalysts with definite cobalt grain sizes, one needs data on the kinetics of $ZrCoH_x$ oxidation, the dynamics of cobalt metal segregation, and the resulting metal particle sizes. In this context, here we studied the magnetization and dynamics of hydrogen removal during the oxidation of $ZrCoH_x$ samples, either intact or after hydrogen thermodesorption.

EXPERIMENTAL

A $ZrCoH_{1.5}$ sample (0.023 g) was placed in a microreactor, which also served as the cell of a vibrational magnetometer. The magnetometer was calibrated against a high-purity cobalt sample. Magnetization was assumed to be proportional to the cobalt metal weight.

The microreactor was connected to a heat conductivity detector in order to continuously measure the gas composition at its outlet. The working gases used were argon (high purity grade), hydrogen free from trace oxygen and water, and O_2 + Ar (5/95).

RESULTS AND DISCUSSION

The $ZrCoH_{1.5}$ oxidation kinetics were studied as follows. First, the hydrogen evolution rate and magnetization for $ZrCoH_x$ were studied in an Ar flow and in an O_2 + Ar (5/95) mixture at a heating rate of 0.5 K/s (Figs. 1, 2).

Intermetallic compound ZrCo has a CsCl-type cubic lattice. Its lattice expands during hydriding along one axis, and $ZrCoH_x$ with $0.3 < x < 3$ crystallizes in an orthorhombic lattice. Four asymmetric octahedral voids and eight symmetric tetrahedral voids appear in the unit cell. There are four formula units in the $ZrCoH_x$ unit cell, and thus hydrogen atoms occupy all voids in

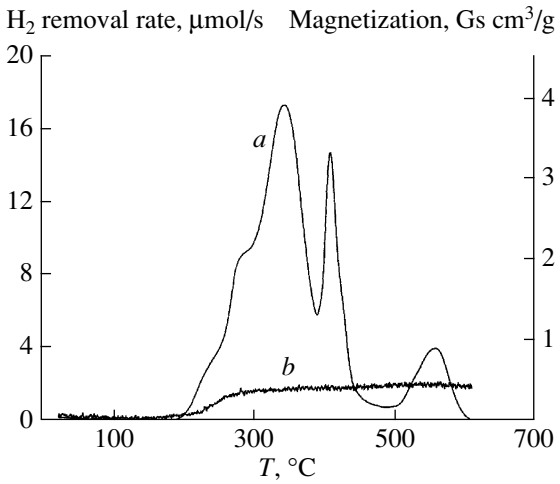

Fig. 1. (*a*) Hydrogen removal rate and (*b*) magnetization vs. temperature for $ZrCoH_{1.5}$ in an argon flow.

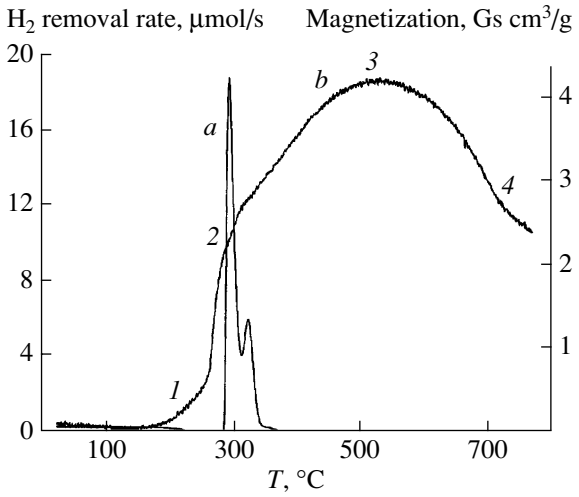

Fig. 2. (*a*) Hydrogen removal rate and (*b*) magnetization vs. temperature for $ZrCoH_{1.5}$ in an O_2 + Ar (5/95) flow.

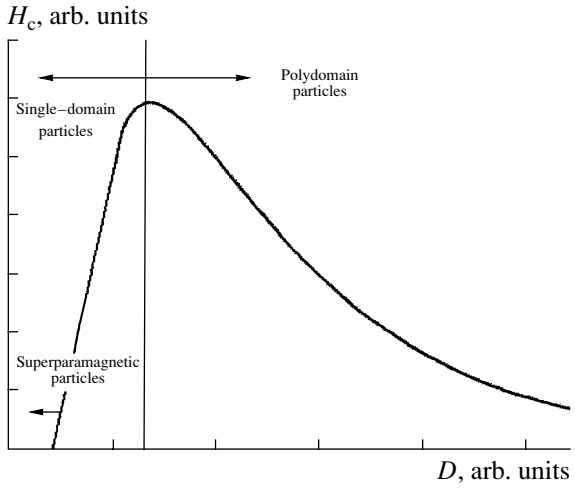

Fig. 3. Qualitative illustration of the coercive force vs. particle size.

$ZrCoH_3$. The hydrogen atoms enclosed in octahedral voids are the first to leave during heating (as demonstrated by both calculations and experiments [2]); the first peak of hydrogen evolution at 340°C is due to this process (Fig. 1, curve *a*). Then, hydrogen atoms leave tetrahedral voids with the second peak appearing at 415°C. The resulting metastable triclinic ZrCoH starts to disproportionate as

$$2ZrCoH \longrightarrow ZrCo_2 + ZrH_2.$$

ZrH_2 decomposition starts only at 515°C (the third peak) and ends only above 600°C. Thus, the full dehydrogenization produces metallic zirconium and a very stable $ZrCo_2$ Laves phase [2].

A weak rise in magnetization can be due to residual oxygen in argon (Fig. 1, curve *b*). Removal of hydrogen by an O_2 + Ar (5/95) flow and the subsequent oxidation of the intermetallic compound (Fig. 2) bring about a far higher rise in magnetization as a result of the oxidative segregation of metallic cobalt. The formation and growth dynamics of cobalt metal particles was studied in the following set of experiments: a sample was heated to a certain temperature (point *1*, *2*, *3*, or *4* in Fig. 2) in an O_2 + Ar (5/95) flow; then, it was cooled to room temperature in an argon flow. For each point, magnetization was measured as a function of field and the coercive force H_c, residual magnetization σ_r, and saturation magnetization σ_s were found by extrapolation to $H \longrightarrow \infty$.

The suggested scheme of $ZrCoH_x$ oxidation is

$$ZrCo_x + O_2 \longrightarrow ZrO_{2-\delta} + Co + H_2O + H_2.$$

The exponential rise in magnetization during the initial oxidation stage at temperatures from 200 to 300°C can be explained by the decomposition of the hydride and the nucleation of metallic cobalt. The rise in the coercive force from point *1* to point *3* is due to the fact that single-domain cobalt crystals are first formed (Fig. 3). The critical single-domain diameter for cobalt particles with uniaxial anisotropy is 20–25 nm [3]. The particles are grown and coarsen as hydride oxidation progresses; the coercive force increases with increasing mean particle size.

The rise in the coercive force from point *3* to point *4* can be interpreted as follows: Co_{met} particles are formed and grown at the initial oxidation stage until temperature reaches 500°C; then, they oxidize and agglomerate; cobalt crystallites are in the single-domain region, and the mean particle diameter decreases and the coercive force rises in the progress of oxidation. It is known [4] that, provided that the system is in the single-domain region, the proportion of superparamagnetic particles is determined by

$$\gamma = 1 - 2\frac{\sigma_r}{\sigma_s}.$$

Here, σ_r is residual magnetization and σ_s is saturation magnetization.

Keeping in mind that the system is in the single-domain region, we calculated the proportion of superparamagnetic particles for points *1*, *2*, and *3* (Table 1).

The proportion of superparamagnetic particles decreases in the progress of oxidation; at 7°C, the limiting size of cobalt superparamagnetic particles is 6.4 nm.

In the second set of experiments, hydrogen was first removed from $ZrCoH_{1.52}$; as a result, a stoichiometric mixture of zirconium and $ZrCo_2$ (contact [Zr + $ZrCo_2$]) was formed. Magnetization rose more significantly during oxidation in these experiments (Fig. 4). Here, as in the first set of experiments, the sample was heated to a certain temperature and cooled to room temperature in an argon flow, after which the hysteresis loop was measured and H_c, σ_s, and σ_r were found. The results of the calculations are listed in Table 2.

Table 1. Magnetic parameters of $[ZrCoH_{1.5}]_{ox}$

Point	σ_s, arb. units	σ_r, arb. units	γ	H_c, Oe
1	1.191	0.262	0.56	77
2	1.042	0.250	0.52	112
3	1.066	0.289	0.46	108
4	1.089	0.324	–	297

Table 2. Magnetic parameters of $[Zr + ZrCo_2]_{ox}$

Point	σ_s, arb. units	σ_r, arb. units	H_c, Oe
1	1.097	0.295	128.5
2	1.072	0.373	143
3	1.079	0.397	436

The most interesting detail is the higher magnetization of the oxidized contact $[Zr + ZrCo_2]_{ox}$ compared to that of the oxidized precursor hydride $[ZrCoH_{1.5}]_{ox}$ at temperatures above 500°C. A likely interpretation of this detail is as follows: $ZrCoH_{1.5}$ oxidation first produces finer cobalt crystallites, which then fully oxidize. In the case of $[Zr + ZrCo_2]$ (in the absence of the hydride system), coarser cobalt particles are initially formed (the system is in the single-domain region except for the initial oxidation stage); these coarser particles do not burn up, because the oxide film stops to grow after reaching a certain thickness. Accordingly, the metal-cobalt proportion and magnetization increase as the temperature rises.

The oxidation kinetics of $ZrCoH_{1.5}$ and $[Zr + ZrCo_2]$ by air were studied in the same manner (Fig. 5). The oxidation of $ZrCoH_{1.5}$ by air radically differs from the oxidation by O_2 + Ar (5/95): magnetization dramatically increases at 275°C because of the instantaneous burning up of all hydride and the elimination of metallic cobalt (some 35% of the possible amount; the rest 65% cobalt is oxidized during hydride burning). The subsequent reduction of $[ZrCoH_{1.5}]_{ox}$ in a hydrogen flow leads to the twofold rise in magnetization (about 70% of the total cobalt is the metal). The coercive force measured for contact *2* (204 Oe) indicates that the system is possibly in the single-domain region and the cobalt particle sizes are comparatively large. The subsequent air oxidation of contact *2* induces a drop in the magnetization, which asymptotically approaches the magnetization of $[ZrCoH_{1.5}]_{ox}$. The cobalt proportion oxidized during hydride burning was apparently enclosed in the ZrO_2 matrix and was not accessible to a hydrogen flow for reduction.

The oxidation kinetics of $[Zr + ZrCo_2]$ in air do not differ from the oxidation kinetics of $[Zr + ZrCo_2]$ in O_2 + Ar (5/95).

The oxidation of $[Zr + ZrCo_2]$ in O_2 + Ar (5/95) induces a more significant rise in magnetization than the oxidation of precursor $ZrCoH_x$ (Fig. 4). We can explain this fact as follows: oxidation first produces larger cobalt particles, which subsequently oxidize by the Cabrera–Mott mechanism and whose oxidation is controlled by oxygen diffusion above 450°C (with the oxidation rate being independent of the oxygen concentration). Accordingly, a significant proportion of cobalt remains in the metallic state. During the oxidation of the precursor hydride by O_2 + Ar (5/95), cobalt nucleation and oxidation progress; the process being

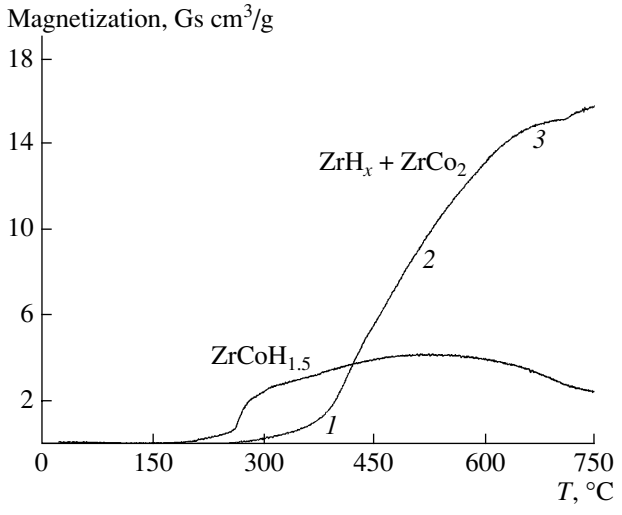

Fig. 4. Cobalt segregation dynamics in the progress of the oxidation of intact $ZrCoH_{1.5}$ and the contact obtained after hydrogen thermodesorption from the hydride.

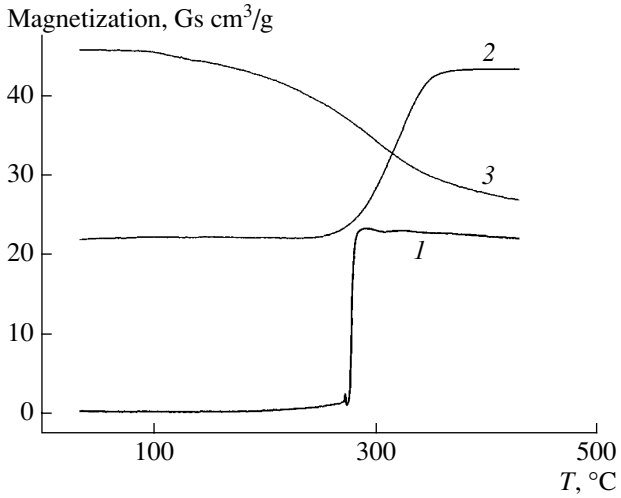

Fig. 5. Cobalt segregation and oxidation dynamics during testing of a $ZrCoH_{1.5}$ sample in air: (*1*) $ZrCoH_{1.5}$ oxidation in air in the temperature-programmed mode (heating at 0.47 K/s) (contact *1*), (*2*) reduction of air-oxidized $ZrCoH_{1.5}$ in a hydrogen flow in the temperature-programmed mode (heating at 0.47 K/s) (contact *2*), and (*3*) oxidation of contact *2* in air in the temperature-programmed mode (heating at 0.47 K/s) (contact *3*).

extended, a significant proportion of cobalt is converted to the oxide by the end of the oxidative treatment.

In summary, the oxidation of [Zr + $ZrCo_2$] is accompanied by a more significant rise in magnetization compared to the precursor $ZrCoH_{1.52}$; coarser Co_{met} particles are produced. The oxidation of $ZrCoH_{1.52}$ by air results in higher magnetizations than the oxidation by O_2 + Ar (5/95), although the oxidation of [Zr + $ZrCo_2$] by air does not significantly differ from oxidation by an O_2 + Ar (5/95) mixture.

REFERENCES

1. Chernavskii, P.A. and Lunin, V.V., *Kinet. Katal.*, 1985, vol. 26, p. 232.
2. Bekris, N., Besserer, U., Sirch, M., and Penzhorn, R.-D., *Fusion Eng. Des.*, vols. 49–50, 2000, p. 781.
3. Petrov, Yu.I., *Fizika malykh chastits* (Physics of Small Particles), Moscow, 1982.
4. Weil, L., *J. Chem. Phys.*, 1954, vol. 51, p. 715.